

Central exclusive dijet production at the Tevatron

Konstantin Goulios

*Experimental High Energy Physics, The Rockefeller University,
1230 York Avenue, New York, NY 10065, USA
dino@fnal.gov*

Received 27 June 2014

Revised 29 July 2014

Accepted 30 July 2014

Published 10 November 2014

We present a review of central exclusive dijet production in $\bar{p}p$ collisions, where the proton and antiproton emerge intact, and only two jets of transverse energy above a certain threshold are present in the final state. The results are published in two papers by the Collider Detector at Fermilab (CDF) Collaboration, a PRL (2000) and a PRD (2008), based on data collected at $\sqrt{s} = 1.8$ TeV and 1.96 TeV, respectively, and a D0 Collaboration paper from studies at 1.96 TeV. In all three cases predictions for the cross-section of Higgs boson production are discussed, a process that proceeds via a similar mechanism as dijet production. Roman Pot Spectrometers equipped with tracking detectors are used to measure the outgoing antiproton (CDF and D0) and proton (D0), and special forward detectors are employed to help reduce backgrounds and enrich the data in diffractive and exclusive dijet events.

Keywords: Exclusive; dijet; Tevatron.

PACS numbers: 13.87.Ce, 12.38.Qk, 12.40.Nn

1. Introduction

We present a review of results on central exclusive dijet production in $\bar{p}p$ collisions at the Tevatron. In this process, both the antiproton and proton survive and a two-jet system (dijet) is centrally produced: $\bar{p} + p \rightarrow \bar{p}' + (\text{jet}_1 + \text{jet}_2) + p'$. Exclusive dijet production is a special case of diffractive dijet production in double Pomeron exchange (DPE), $\bar{p} + p \rightarrow [\bar{p}' + \mathbb{P}_{\bar{p}}] + [p' + \mathbb{P}_p] \rightarrow \bar{p}' + X + p'$, where \mathbb{P} designates a Pomeron, defined as an exchange of a colorless combination of gluons and/or quarks carrying the quantum numbers of the vacuum, and X is a system that includes the jets. We cover two Collider Detector at Fermilab (CDF) papers, a PRL (2000)¹ and a PRD (2008),² which are based on data collected at $\sqrt{s} = 1.8$ TeV and 1.96 TeV, respectively, as well as a D0 Collaboration study at $\sqrt{s} = 1.96$ TeV.³ The CDF

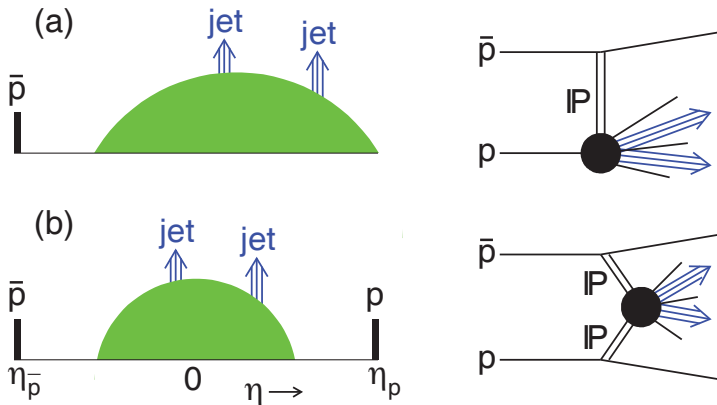


Fig. 1. Illustration of event topologies in pseudorapidity, η , and associated Pomeron-exchange diagrams for dijet production in (a) single diffraction and (b) DPE; the shaded areas at left represent underlying-event particles not associated with the jets (from Ref. 1).

PRD (2008) reports the first observation of the exclusive dijet production process, while in the CDF PRL (2000) an upper limit is set, which was important at the time of publication as it excluded models that predicted much larger cross-sections, see e.g. Ref. 4. The D0 paper reports results for a high dijet invariant mass, which are complementary to those of CDF.

In a particle-like Pomeron picture,⁵ the system X is produced by the collision of two Pomerons, $\mathbb{P}_{\bar{p}} + \mathbb{P}_p \rightarrow X$, where in addition to the two jets the final state generally contains Pomeron remnants: $X \equiv Y_{\mathbb{P}/\bar{p}} + (\text{jet}_1 + \text{jet}_2) + Y_{\mathbb{P}/p}$. In this figure, exclusivity is defined as the absence of Pomeron remnants.

Dijet production in DPE is a sub-process to dijet production in single diffractive (SD) dissociation, where only the antiproton (proton) survives while the proton (antiproton) dissociates. Figure 1 shows schematic diagrams for SD and DPE dijet production along with the event topology in pseudorapidity space (from Ref. 1). In SD, the escaping \bar{p} is adjacent to a rapidity gap, defined as a region of pseudorapidity devoid of particles.^a In DPE, two such rapidity gaps are present.

Dijet production may occur exclusively in DPE^b via a fluctuation of the Pomeron remnants down to zero, or with a much higher cross-section in models in which the Pomerons are treated as partons and the dijet system is produced in a $2 \rightarrow 2$ process analogous to $\gamma\gamma \rightarrow \text{jet} + \text{jet}$.⁶ In a special case, exclusive dijets may be produced through an intermediate state of a Higgs boson decaying into $\bar{b}b$, $\mathbb{P}_{\bar{p}} + \mathbb{P}_p \rightarrow H^0 \rightarrow (\bar{b} \rightarrow \text{jet}_1) + (b \rightarrow \text{jet}_2)$.

^aRapidity, $y = \frac{1}{2} \ln \frac{E+p_L}{E-p_L}$, and pseudorapidity, $\eta = -\ln \tan \frac{\theta}{2}$, are used interchangeably for particles detected in the calorimeters, since in the kinematic range of interest in this analysis they are approximately equal.

^bWhile the exclusive DPE process is part of the inclusive, it has become traditional to refer to the processes with and without Pomeron remnants as “inclusive” and “exclusive,” respectively. In this paper, we will follow this tradition.

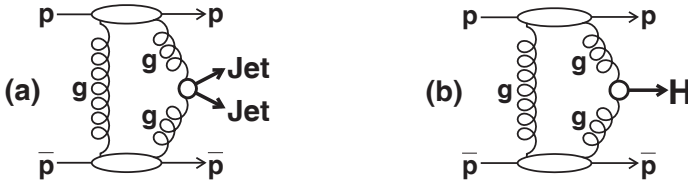


Fig. 2. LO diagrams for exclusive production of (a) dijet and (b) Higgs in $\bar{p}p$ collisions.

Finally, exclusive production may also occur through a t -channel color singlet two-gluon exchange at leading order (LO) in perturbative quantum chromodynamics (QCD), as shown schematically in Fig. 2(a), where one of the two gluons takes part in the hard scattering that produces the jets, while the other neutralizes the color flow.⁷ A similar diagram, Fig. 2(b), is used in Ref. 7 to calculate exclusive Higgs boson production.

Predictions for dijet production are generally hampered by large uncertainties due to nonperturbative suppression effects associated with the rapidity gap survival probability. As these effects are common to exclusive dijet and Higgs production mechanisms, the measurement of exclusive dijet production could provide a benchmark against which to calibrate the available theoretical models.^{7,8}

2. CDF Results

Measurement strategy. The exclusive signal is extracted using the “dijet mass fraction” method to minimize detector-dependent effects.¹ From the energies and momenta of the jets in an event, the ratio $R_{jj} \equiv M_{jj}/M_X$ of the dijet mass M_{jj} to the total mass M_X of the final state system (excluding the \bar{p} and p) is formed and used to discriminate between the signal from an exclusive dijet system, expected to appear at $R_{jj} \sim 1$, and the background from inclusive DPE dijets, expected to have a continuous distribution concentrated at lower R_{jj} values. Because of smearing effects in the measurement of E_T^{jett} and η^{jett} and gluon radiation from the jets, the exclusive dijet peak is broadened and shifted to lower R_{jj} values. Therefore, the exclusive signal is obtained by a fit of the R_{jj} distribution to expected signal and background shapes generated by Monte Carlo (MC) simulations.

In the PRD (2008) analysis,² the background shape is checked with an event sample of heavy quark flavor dijets, for which exclusive production is expected to be suppressed in LO QCD by the $J_z = 0$ selection rule of the hard scattered digluon system, where J_z is the projection of the total angular momentum of the system along the beam direction.⁹

The CDF detector relevant to the PRL (2000) analysis is described in Ref. 10. It was upgraded to accommodate the much higher instantaneous luminosities of the run in which the data for PRD (2008) were collected. The upgraded detector is shown in Fig. 3.¹¹ The main changes relevant to diffractive physics are the replacement of the beam–beam counter (BBC) scintillation-counter array ($3.2 < |\eta| < 5.9$,

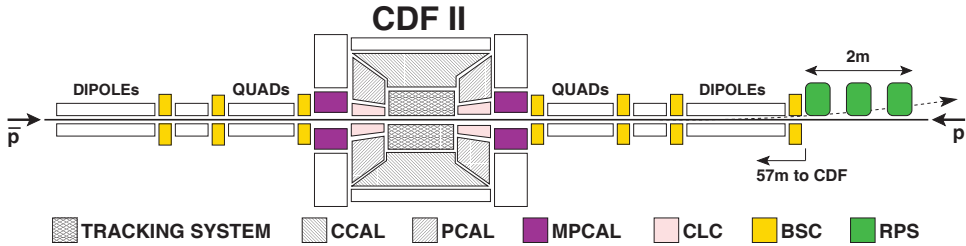


Fig. 3. Schematic drawing of the CDF II detector and beam layout (Ref. 11).

not shown in Fig. 3), by the Cherenkov Luminosity Counters (CLC, $3.7 < |\eta| < 4.7$), and the addition of the MiniPlug calorimeters (MPCAL, $3.6 < |\eta| < 5.2$).¹² The MPCALs were designed to measure the energy and lateral position of particles, and provide discrimination between hadron- and electron-induced showers. For a detailed description of the forward detector components relevant to the PRD (2008) data analysis, see Ref. 13.

PRD (2000) results. The absolute DPE dijet cross-section is obtained by multiplying the DPE/SD event ratio by the SD dijet cross-section, which is normalized by scaling to the measured¹⁶ inclusive (soft) cross-section of 0.78 ± 0.16 mb. For $0.035 < \xi_{\bar{p}} < 0.095$, $0.01 < \xi_p < 0.03$, $|t_{\bar{p}}| < 1$ GeV² and jets of $E_T > 7$ [$E_T > 10$] GeV confined within $-4.2 < \eta < 2.4$, we obtain $\sigma^{\text{DPE}} = 43.6 \pm 4.4(\text{stat}) \pm 21.6(\text{syst})$ [$3.4 \pm 1.0(\text{stat}) \pm 2.0(\text{syst})$] nb, where the systematic errors are dominated by the uncertainties in normalization (20%) and jet energy calibration (40%). In terms of an absolute cross-section, the 95% C.L. upper bound for events in which the jet energies could account for the total energy of the central system (exclusive candidates) corresponds to 3.7 nb. Theoretical estimates of this cross-section range from $\sim 10^3$ times larger⁴ to a few times smaller¹⁷ values than the measured upper bound.

PRD (2008) results. Three data samples are used in the analysis, referred to as the DPE, SD and nondiffractive (ND) event samples. The exclusive dijet signal is extracted from the DPE event sample, while the SD and ND samples are used for evaluating backgrounds. The total integrated luminosity of the DPE sample is 312 ± 19 pb⁻¹.

Heavy flavor quark jets. At high energies the dijet mass fraction is dominated by the parton level process $gg \rightarrow gg$, as contributions from $gg \rightarrow q\bar{q}$ are suppressed. Born level cross-sections for exclusive production of a color-singlet dijet system of mass M are suppressed by a factor $(m_q^2/M^2)(1 - 4m_q^2/M^2)$,¹⁴ which vanishes as $m_q^2/M^2 \rightarrow 0$ ($J_z = 0$ selection rule⁹). Exclusive $gg \rightarrow q\bar{q}$ contributions are also strongly suppressed in NLO and NNLO QCD, and in certain higher orders.¹⁵

To ensure a quark origin, CDF selected jets from heavy flavor (HF) b - or c -quarks, identified from secondary vertexes produced from the decay of intermediate B - or D -mesons using the SVX II detector. Both b - and c -quark jets are used, since the suppression mechanism holds for all quark flavors.

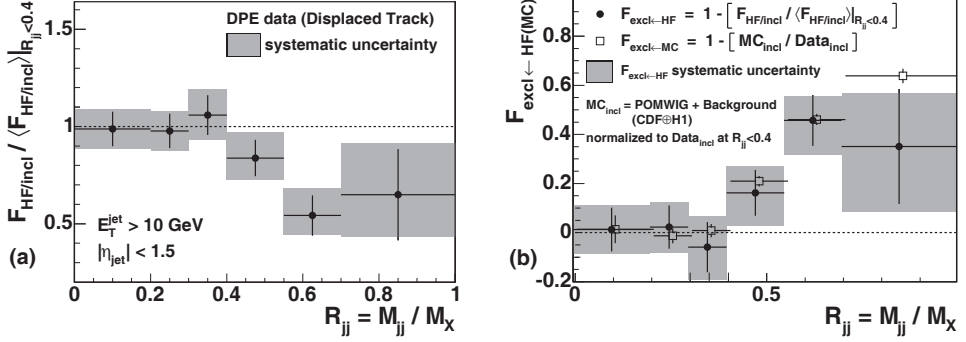


Fig. 4. (a) Measured ratio $F_{\text{HF}/\text{incl}}$ of HF to inclusive jets of $E_T^{\text{jet}} > 10 \text{ GeV}$ and $|\eta_{\text{jet}}| < 1.5$ as a function of dijet mass fraction R_{jj} , normalized to the weighted average value within $R_{jj} < 0.4$; (b) values of $F_{\text{excl} \leftarrow \text{HF}} = 1 - F_1$ (filled circles) and $F_{\text{excl} \leftarrow \text{MC}} = 1 - F_2$ (open squares) versus R_{jj} , where $F_1 = F_{\text{HF}/\text{incl}} / \langle F_{\text{HF}/\text{incl}} \rangle_{R_{jj} < 0.4}$, which is plotted in (a) versus R_{jj} , and F_2 is the ratio of POMWIG MC to inclusive dijet events.

Results. Selected results are summarized in Figs. 4 and 5 for events with jets of $E_T^{\text{jet}} > 10 \text{ GeV}$ and $|\eta_{\text{jet}}| < 1.5$. Figure 4 shows the evidence for a suppression of the HF component in the inclusive jet event sample as predicted in Ref. 14. Figure 5 (left) presents the measured total exclusive dijet cross-section versus the minimum E_T^{jet} of the two jets compared to EXHUME and EXCLDPE predictions. The data clearly favor EXHUME. Using EXHUME to generate events, selecting a generated event sample that maps the selection criteria of the events in Fig. 5 (left), and reconstructing them exactly in the same way as the real events, the measured cross-sections are converted to an exclusive dijet differential cross-section at the hadron level,² Fig. 5 (right). This distribution supports the EXHUME prediction, and thereby the perturbative QCD calculation on which EXHUME is based.¹⁸ It therefore constrains the predictions for exclusive Higgs boson production.

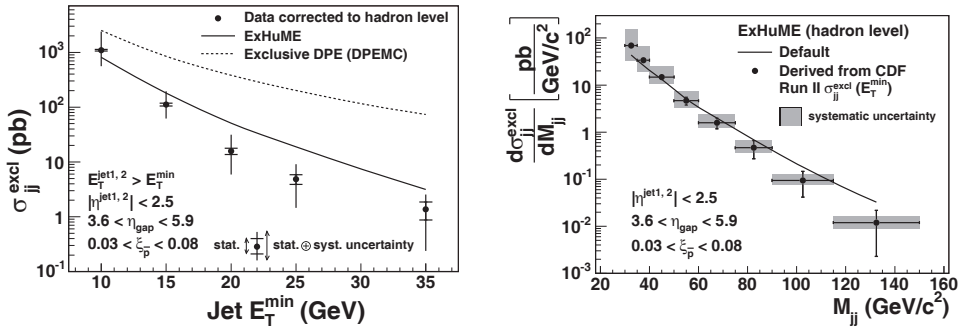


Fig. 5. (Left) The total exclusive dijet cross-section for events with $E_T^{\text{jet}} > 10 \text{ GeV}$ and $|\eta_{\text{jet}}| < 1.5$ plotted versus the minimum E_T^{jet} of the two jets compared to EXHUME and EXCLDPE predictions; (Right) EXHUME exclusive dijet differential cross-section at the hadron level versus dijet mass M_{jj} .

3. D0 Results

The data used in this analysis were collected with the D0 detector in the period between August 2002 and April 2006 at the Tevatron Collider at a center-of-mass energy $\sqrt{s} = 1.96$ TeV. The D0 detector is described in detail in Ref. 19. For this analysis, the most relevant components are the central and forward calorimeters used for jet reconstruction and the identification of a rapidity gap devoid of any energy (above noise) in the calorimeter, respectively. The D0 liquid argon and uranium calorimeter is divided in three parts housed in independent cryostats covering the following regions in pseudorapidity (see footnote a): $|\eta| < 1.1$ (central calorimeter) and $1.6 < |\eta| < 4.2$ (two forward calorimeters). Jets in Exclusive Double Pomeron (EDP) events are expected to be more central than in other jet production processes, therefore both jets are required to be central with a rapidity $|y| < 0.8$, where the rapidity is defined as $y = \frac{1}{2} \ln(E + p_z)/(E - p_z)$ where E is the jet energy and p_z is the momentum component of the jet along the beam axis. The forward region of the calorimeter is used to check for the presence of a rapidity gap on each side of the dijet system. Leading protons were not detected, so diffraction dissociation is included. D0 introduced a parameter Δ (see Ref. 3) expected to be $\Delta \sim 0.85$ –1.0 for exclusive dijets.

Data were collected using an inclusive jet trigger requiring at least one jet in an event to be above a p_T threshold of 45 GeV in uncorrected energy, in order to select exclusive diffractive events for dijet invariant mass above 100 GeV.

Pseudo experiments used to determine the significance of the EDP signal include variations over each systematic uncertainty. The observed significance corresponds to the fraction of outcomes that yield an EDP cross-section at least as large as that measured in data. Seven bins are used as input for the significance calculation: six bins for Δ between 0.1 and 0.85, where the predominant region used in the MC normalization is removed, and the $\Delta \geq 0.85$ bin. Figure 6 displays the dijet invariant mass distribution for $\Delta \geq 0.85$.

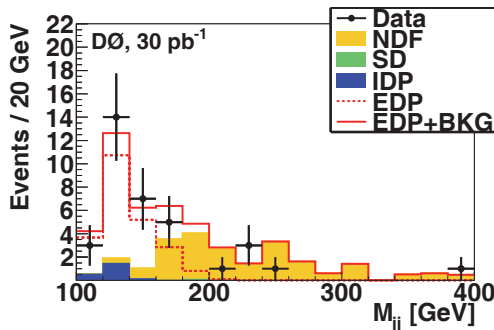


Fig. 6. Dijet invariant mass distribution for stacked MC (NDF, SD and IDP) and data after applying the requirement on $\Delta \geq 0.85$ (see text). The EDP distribution is shown without adding the stacked background.

In summary, the D0 PRL paper presents evidence at the 4.1 standard deviation level for events consistent with the exclusive dijet production topology in $p\bar{p}$ collisions at a center-of-mass energy $\sqrt{s} = 1.96$ TeV at high dijet invariant mass ($M_{jj} > 100$ GeV). These were the highest mass states directly studied for exclusive production in hadron colliders at the time of publication.

Acknowledgments

I would like to thank Dr. Murilo Rangel for kindly providing me with information regarding the D0 study on exclusive dijet production and granting permission to use the D0 figure in this summary. I also thank my CDF colleagues for their contributions that made this work possible, and the Office of Science of the Department of Energy and the Rockefeller University for their generous financial support.

References

1. CDF Collab. (T. Affolder *et al.*), *Phys. Rev. Lett.* **85**, 4215 (2000).
2. CDF Collab. (A. Aaltonen *et al.*), *Phys. Rev. D* **77**, 052004 (2008).
3. D0 Collab. (V. M. Abazov *et al.*), *Phys. Lett. B* **705**, 193 (2010).
4. A. Berera, *Phys. Rev. D* **62**, 014015 (2000).
5. G. Ingelman and P. Schlein, *Phys. Lett. B* **152**, 256 (1985).
6. A. Bialas and P. V. Landshoff, *Phys. Lett. B* **256**, 540 (1991).
7. V. A. Khoze, A. D. Martin and M. G. Ryskin, *Eur. Phys. J. C* **14**, 525 (2000).
8. M. Boonekamp, R. Peschanski and C. Royon, *Phys. Lett. B* **598**, 243 (2004).
9. V. A. Khoze, A. D. Martin and M. G. Ryskin, *Eur. Phys. J. C* **19**, 477 (2001) [Erratum: *ibid.* **20**, 599 (2001)].
10. F. Abe *et al.*, *Nucl. Instrum. Methods Phys. Res. A* **271**, 387 (1988).
11. CDF Collab. (D. Acosta *et al.*), *Phys. Rev. D* **71**, 032001 (2005).
12. M. Gallinaro *et al.*, *Nucl. Instrum. Methods A* **496**, 333 (2003).
13. K. Goulianos, Diffraction at the Tevatron: CDF results, in *Proc. DIFFRACTION 2006, Int. Workshop on Diffraction in High-Energy Physics*, Adamantas, Milos Island, Greece, September 2006, *PoS (DIFF2006)*, p. 016.
14. V. A. Khoze, A. D. Martin and M. G. Ryskin, *Eur. Phys. J. C* **23**, 311 (2002).
15. V. A. Khoze, M. G. Ryskin and W. J. Stirling, *Eur. Phys. J. C* **48**, 477 (2006).
16. F. Abe *et al.*, *Phys. Rev. D* **50**, 5550 (1994).
17. V. A. Khoze, A. D. Martin and M. G. Ryskin, arXiv:hep-ph/0006005.
18. A. B. Kaidalov, V. A. Khoze, A. D. Martin and M. G. Ryskin, *Eur. Phys. J. C* **31**, 387 (2003); *ibid.* **33**, 261 (2004).
19. D0 Collab. (V. M. Abazov *et al.*), *Nucl. Instrum. Methods Phys. Res. A* **565** (2006).